Optical single-sideband modulation based on a silicon dual-parallel Mach-Zehnder modulator

Panpan Shi, Liangjun Lu*, Gangqiang Zhou, Shuhuang Chen, Jianping Chen, and Linjie Zhou
State Key Laboratory of Advanced Optical Communication Systems and Networks, Department of Electronic Engineering, Shanghai Jiao Tong University, Shanghai, China
luliangjun@sjtu.edu.cn

Abstract: We experimentally demonstrate optical single-sideband modulation with a variable RF frequency. The sideband suppression ratio for the carrier-remained and carrier-suppressed modulation is more than 38 dB and 13 dB from 1 to 24 GHz, respectively.
OCIS codes: (250.5300) photonic integrated circuits; (250.7360) waveguide modulators; (130.0250) optoelectronics

1. Introduction

Optical single-sideband modulation (SSB) has wide applications in high-speed broadband wireless communications, microwave photonics signal processing, and light detection and ranging (LiDAR). In a radio-over-fiber (RoF) system, the employment of optical SSB modulation can improve the spectral efficiency and mitigate the chromatic dispersion issue [1, 2]. Optical SSB modulation in combination with a narrow-bandwidth optical filter can also implement a tunable microwave photonic filter [3]. Nowadays, frequency-modulated continuous waveform (FMCW) LiDAR systems are receiving increasing attention in both academia and industry. Compared to the time-of-flight detection, FMCW system improves the receiver sensitivity due to the coherent amplification. Linear optical FMCW signal can be generated by modulating the laser light with a suppressed-carrier SSB modulator [4].

Several silicon optical SSB modulators have been demonstrated using different structures, such as a dual-parallel ring modulator [5], an electro-optic modulator with a ring-based notch filter [6], and a planar-Bragg-grating-based optical Hilbert transformer [7]. In this paper, we present the experimental demonstration of optical single-sideband modulation with both remained carrier (SSB-C) and suppressed carrier (SSB-SC) using a dual-parallel Mach-Zehnder modulator (DP-MZM) on the silicon photonics platform.

2. Device structure and working principle

Figure 1(a) shows the schematic structure of the silicon DP-MZM. It consists of a parent Mach-Zehnder interferometer (MZI) with two nested child MZMs in the two arms. Each child MZM contains a 3-mm-long single-drive push-pull traveling wave electrode (TWE) and two 50-μm-long thermo-optic (TO) phase shifters (PS_1-PS_4). There is an additional phase shifter (PS_5) integrated in the bottom arm of the parent MZI. The modulation is based on free-carrier depletion of lateral PN junctions embedded in the arms of the child MZMs. The device is designed to work for transverse-electric (TE) polarized light. Multimode interference (MMI) couplers are utilized to form the optical power splitters and combiners [8]. The width and length of the MMI couplers are 3.4 μm and 10 μm, respectively. The device was fabricated with complementary metal-oxide-semiconductor (CMOS) compatible processes. Figure 1(b) shows the microscope image of the DP-MZM. All the DC pads are wire-bonded to a printed circuit board (PCB) for TO phase tuning of the waveguides and reverse bias of the PN junctions. The footprint of the modulator is 5.8 mm × 1.0 mm.

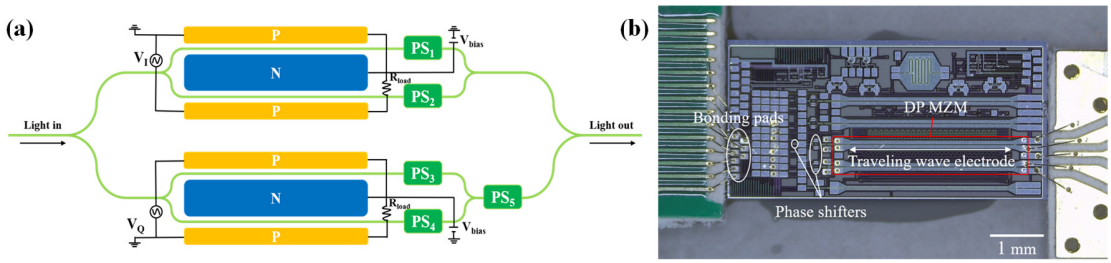

Fig. 1. (a) Device structure of the DP-MZM. (b) Microscope image of the fabricated DP-MZM.

Figure 2 illustrates the device working principle. For both SSB-C and SSB-SC modulation, the input RF signal is first divided into two branches with the same magnitude but a 90° phase difference by a quadrature hybrid coupler. These two RF signals are then applied to the two child MZMs. The phase difference of two arms in the parent MZI is tuned to 90° with PS_5. To generate the optical SSB-C signal, the two child MZMs work at the quadrature point, where

the phase difference of the child MZM arms is π/2. Therefore, each child MZM generates two sidebands besides the optical carrier. The lower sideband (LSB) from the top MZM is π-phase different from that of the bottom one. At the output port, the LSB is therefore suppressed, generating the optical SSB-C signal. For SSB-SC modulation, these two child MZMs are tuned to the null-transmission point, where the phase difference becomes π. In that case, the optical carrier is suppressed, generating the optical SSB-SC signal.

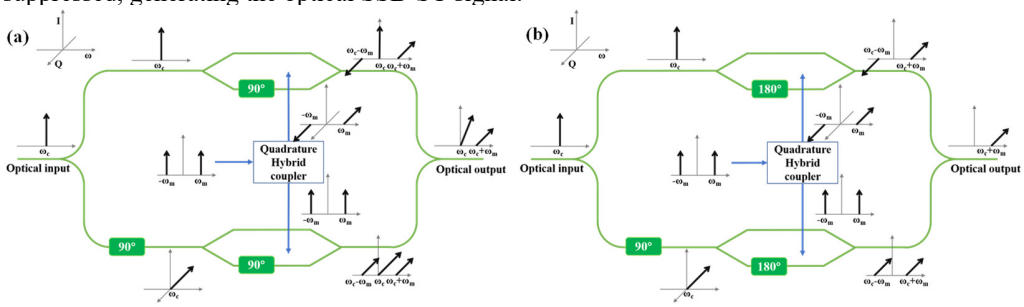

Fig. 2. Device configuration and working principle for (a) SSB-C and (b) SSB-SC modulations.

3. Experimental results

Figure 3(a) shows the experimental setup. The RF signal generated by a microwave signal generator (Keysight, N5183B) is first fed into a quadrature hybrid coupler and split into two RF signals with a phase difference of 90°. The two RF signals are amplified by two microwave amplifiers and then applied onto the DP-MZM using a GSGSG RF probe. Multi-channel voltage sources are used to adjust the phase of each arm and set the PN junctions to reverse bias. The optical spectrum of the modulated signal from the DP-MZM is measured by an optical spectrum analyzer (OSA, APEX AP2040A).

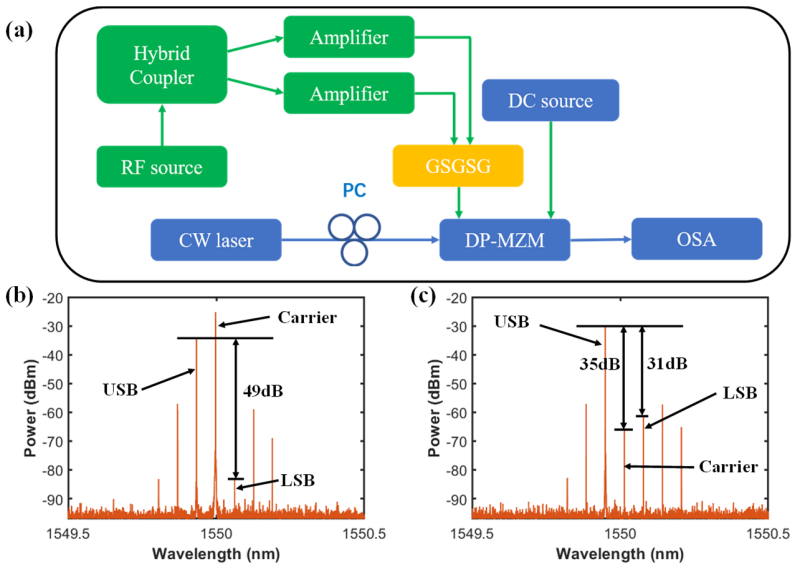

Fig. 3. (a) Experimental setup for measuring the SSB modulation. (b, c) Measured optical spectra for (b) the SSB-C modulation and (c) the SSB-SC modulation.

The frequency of the input RF signal is first set at 8 GHz. After the hybrid coupler and two microwave amplifiers, the power of the two quadrature RF signals is 26 dBm. The continuous wave (CW) laser wavelength is set at 1550 nm. By properly adjusting the voltage applied to the phase shifters, we can get the SSB-C signal. Figure 3(b) shows the measured optical spectrum of the SSB-C signal. We can see that the LSB of the modulated signal is successfully suppressed while the upper sideband (USB) remains high. The measured SSR is 49 dB. Then, we change the voltage on the phase shifters and set the DP-MZM at the SSB-SC mode. The input RF signal and laser light are the same as the SSB-C modulation. Figure 3(c) shows the optical SSB-SC modulation result. The SCSR is 35 dB and the SSR is 31 dB. We attribute the relatively low SSR and SCSR to the limited extinction ratio and the unequal modulation

efficiency of the top and bottom MZMs. For SSB-C modulation, the SSR can be optimized by tuning the phase difference of the two child MZM to obtain an equal amplitude of LSBs. However, for SSB-SC modulation, it is much difficult to balance the amplitudes of both carrier and LSB of these two child MZMs simultaneously. Therefore, the SSR of SSB-SC modulation is lower than that of SSB-S modulation.

We next measure the SSB-C and the SSB-SC modulation across a RF frequency range from 1 GHz to 40 GHz. Figures 4(a) and 4(c) show the measured optical spectra of the SSB-C and SSB-SC signals with various RF frequencies. The extracted SSR of the optical SSC-C signals as a function of RF frequency is illustrated in Fig. 4(b). The measured SSR is higher than 38 dB when the input RF signal frequency is lower than 34 GHz, and is higher than 28 dB across the 1-40GHz frequency range. Figure 4(d) shows the extracted SSR and SCSR of the SSB-SC modulation as a function of RF frequency. Due to the limited bandwidth of the modulator, the amplitudes of the generated sidebands decrease with the RF frequency. Thus, the SSR and the SCSR are degraded to 13 dB and 14 dB, respectively, when the input RF frequency is 24 GHz.

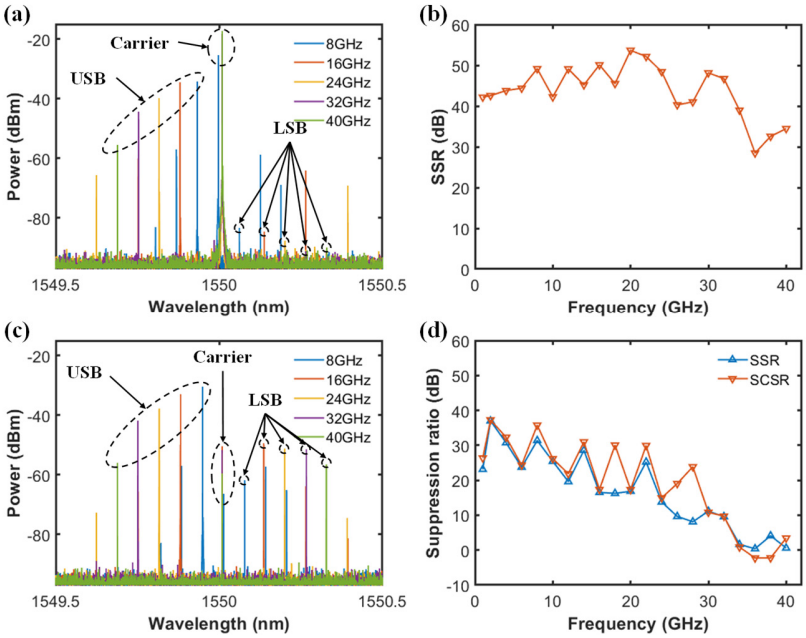

Fig. 4. Measured optical spectra for (a) SSB-C and (c) SSB-SC modulations when the RF signal frequency changes from 8 GHz to 40 GHz. (b) Extracted SSR for the SSB-C modulation. (d) Extracted SSR and SCSR for the SSB-SC modulation.

3. Conclusion

We have demonstrated optical SSB-C and SSB-SC modulations based on a silicon DP-MZM. For SSB-C modulation, the measured SSR is larger than 38 dB when the modulation frequency is lower than 34 GHz. For SSB-SC modulation, the SSR is better than 13 dB and the SCSR is better than 14 dB in the RF frequency range of 1 GHz to 24 GHz. These results show that the silicon DP-MZM is a promising device to generate optical SSB signals.

References

[1] Smith G H, Novak D, Ahmed Z, "Technique for optical SSB generation to overcome dispersion penalties in fibre-radio systems," Electronics Letters, **33,** 74-75 (1997).
[2] Frankel M Y, Esman R D, "Optical single-sideband suppressed-carrier modulator for wide-band signal processing," Journal of Lightwave Technology **16**, 859(1998).
[3] Sagues M, Olcina R G, Loayssa A, et al., "Multi-tap complex-coefficient incoherent microwave photonic filters based on optical single-sideband modulation and narrow band optical filtering," Optics Express **16**, 295-303 (2008).
[4] Gao S, Hui R, "Frequency-modulated continuous-wave lidar using I/Q modulator for simplified heterodyne detection," Optics Letters **37**, 2022-2024 (2012).
[5] Yu B M, Lee J M, Mai C, et al., "Single-chip Si optical single-sideband modulator," Photonics Research **6**, 6-11 (2018).
[6] Song S, Yi X, Chew S X, et al., "Optical single-sideband modulation based on silicon-on-insulator coupled-resonator optical waveguides," Optical Engineering **55**, 031114 (2015).
[7] Sima C, Gates J C, Rogers H L, et al., "Phase controlled integrated interferometric single-sideband filter based on planar Bragg gratings implementing photonic Hilbert transform," Optics Letters **38**, 727-729 (2013).
[8] Zhu H, Zhou L, Wang T, et al., "Optimized silicon QPSK modulator with 64-Gb/s modulation speed," IEEE Photonics Journal **7**, 1-6 (2015).